

Symmetry analysis of Raman scattering mediated by neighboring molecules

Mathew D. Williams, David S. Bradshaw and David L. Andrews^{a)}

School of Chemistry, University of East Anglia, Norwich NR4 7TJ, United Kingdom

Raman spectroscopy is a key technique for the identification and structural interrogation of molecules. It generally exploits changes in vibrational state within individual molecules which produce, in the scattered light, frequencies that are absent in the incident light. Considered as a quantum optical process, each Raman scattering event involves the concurrent annihilation and creation of photons of two differing radiation modes, accompanying vibrational excitation or decay. For molecules of sufficiently high symmetry, certain transitions may be forbidden by the two-photon selection rules, such that corresponding frequency shifts may not appear in the scattered light. By further developing the theory on a formal basis detailed in other recent work [*J. Chem. Phys.* **144**, 174304 (2016)], the present analysis now addresses cases in which expected selection rule limitations are removed as a result of the electronic interactions between neighboring molecules. In consequence, new vibrational lines may appear – even some odd parity (*ungerade*) vibrations may then participate in the Raman process. Subtle differences arise according to whether the input and output photon events occur at either the same or different molecules, mediated by intermolecular interactions. For closely neighboring molecules, within near-field displacement distances, it emerges that the radiant intensity of Raman scattering can have various inverse-power dependences on separation distance. A focus is given here to the newly permitted symmetries, and the results include an extended list of irreducible representations for each point group in which such behavior can arise.

I. INTRODUCTION

Raman scattering is a well-known analytical tool in modern spectroscopy and microscopy.¹⁻⁴ At the fundamental level, it is an inelastic scattering technique that generates photons with a slightly different energy from the input. Such differences usually correspond to transitions between vibrational levels, while the electronic states stay the same. In recent work⁵ we have developed a framework of quantum electrodynamics (QED)^{6, 7} to address Raman scattering influenced by a second, neighboring molecule; this is one of many situations in which such a theory of fundamental coupling is applied.⁸⁻¹⁶ Our interest is not only in the modification of line intensities (beyond the familiar heterogeneous spectral broadening): we have shown that it is possible to engender additional spectra lines that are not conventionally Raman active, identifying the constraints that apply. The symmetry aspects of the latter feature are the focus of the present work. The origin of this effect lies in two-center near-field coupling that involves the scattering of light by the molecular pair with a single or double virtual photon exchange between them. This form of interaction is responsible for a wide range of other effects in the field of chemical physics,¹⁷ most notably resonant energy transfer (where the input photon annihilation and output creation events are necessarily on different sites). A similar type of coupling can be exploited to enhance second order hyperpolarizabilities, in which connection such an interaction is referred to as cascading.¹⁸ Our present results lead to a detailed analysis on the symmetry constraints and selection rules governing the emergence of proximity-induced Raman signals.

In the next section, a very brief overview of the fundamental theory is provided, primarily to introduce the molecular properties whose symmetry analysis reveals the new selection rules. This is followed by an in-depth analysis of the wide-ranging cases that generate Raman-forbidden spectra lines, leading to a systematic listing based on the standard Schoenflies designations for the molecular point groups. The penultimate section provides a few indicative examples, and the general applicability of this work is discussed in the Conclusion.

II. KEY ELEMENTS OF THE PAIR COUPLING

It is appropriate to begin with an expression, whose detailed derivation has been presented previously,⁵ for the radiant intensity, I' , for Raman emission into a solid angle Ω' , from a molecule A , incorporating all of the fundamentally permissible contributory mechanisms associated with the electronic influence of a neighboring molecule B :

$$I'(\Omega') = \left(\frac{k'^2}{4\pi\epsilon_0} \right)^2 I_0 \times \left| \underbrace{M_{FI}^A + M_{FI}^{A|B'} + M_{FI}^{B|A'} + M_{FI}^{A|B} + M_{FI}^{B|A}}_0 + \underbrace{M_{FI}^{A||B'} + M_{FI}^{B||A'} + M_{FI}^{A||B} + M_{FI}^{B||A}}_2 + \dots \right|^2, \quad (1)$$

where the first matrix element M_{FI}^A involves only molecule A and is the single-center term that corresponds to conventional

^{a)}david.andrews@physics.org

Raman scattering. Using standard Feynman time-ordered representations, the most widely deployed diagrammatic methodology,¹⁹ one photon arrives and another departs from a world-line for molecule A , and the interpretation leads to a matrix element that engages the standard transition polarizability for the molecule. The successive terms appearing in two underbraces in Equation (1) then collect all terms that relate to a specific number of virtual photon exchanges between the world-lines of molecule A and B ,⁷ one and two respectively: it is these eight terms that are of interest in this paper, and they will be referred to sequentially as couplings (i) through (viii). Each represents a unique set of interactions that can occur between the two molecules, as indicated by the arrangement of symbols in the superscripts: the leftmost character signifies the site of photon annihilation, with the prime denoting the molecule where the radiation mode is created, and the number of vertical bars corresponds to the number of virtual photons exchanged. Coupling (i), represented by $M_{FI}^{A|B'}$, has the annihilation at molecule A and creation at molecule B , with a single virtual photon connecting the pair, as illustrated in Fig. 1(a); (ii), indicated by $M_{FI}^{B|A'}$, is where the roles of A and B in (i) are interchanged, i.e.

the radiation mode is annihilated at B and created at A ; (iii) $M_{FI}^{A|B}$ is a contribution corresponding to photon annihilation and creation at A , as with conventional Raman, but including a single additional coupling to molecule B , as seen in Fig. 1(b); (iv) $M_{FI}^{B|A}$ is essentially as in (iii) but with $A \leftrightarrow B$: the radiation modes are both annihilated and created at molecule B . Inspecting the final four couplings, (v)-(viii), it can be seen that the corresponding matrix elements are identical to the first four cases except for one addition: a second solidus, which indicates an additional virtual photon exchange between the pair of molecules. Fig. 1(c) and Fig. 1(d) provide Feynman visualizations for couplings (v) and (vii), respectively.

This exhausts the possibilities for the complete set of spatial locations for the interactions, but not the temporal arrangement of those interactions: since the initial and final states are the only experimentally discernible states, each matrix element subsumes a summation of all radiation modes and permutations of intermediate states and interaction events. The explicit form for each matrix elements are given by Equations (3), (11), (12), (15), (16), (19), (20), (24), and (25) in our previous publication.⁵

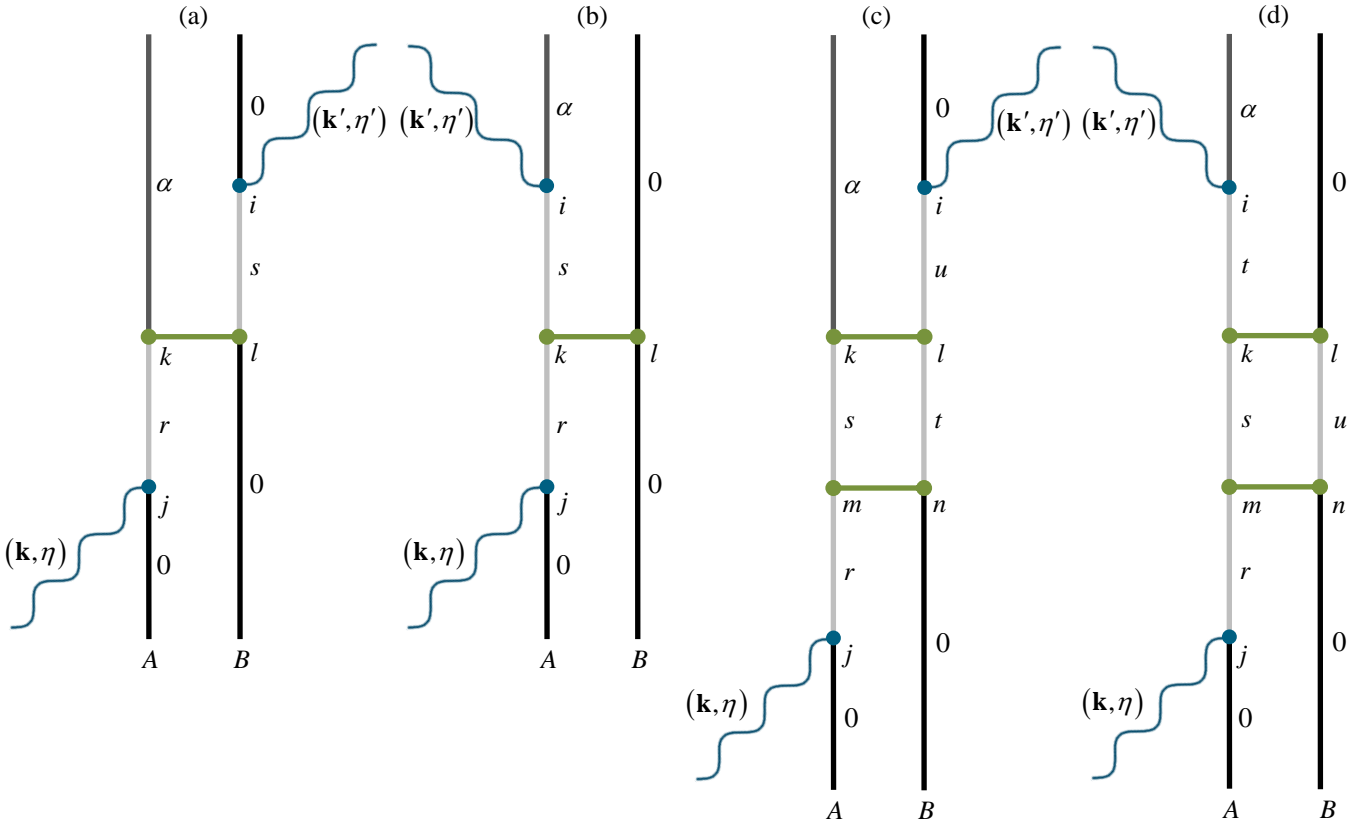


FIG. 1. An illustrative permutation of interactions and time evolution of molecules A and B in Feynman diagrammatic representations for four types of interaction, detailed in the main text. Sinusoidal lines indicate detectable photons (of wavevector $\mathbf{k}^{(\prime)}$ and polarization $\eta^{(\prime)}$), a horizontal line depicts a near-zone virtual photon exchange. Each character $\{r, s, t, u\}$ corresponds to an intermediate (virtual) state of the molecule, between interactions denoted by Cartesian indices $\{i, j, k, l, m, n\}$. Each of these Feynman graphs is a representative of a set with permuted time-orderings.

All matrix elements that contribute to the radiant intensity, equation (1), have a number of virtual photon exchanges. In the near-field static limit each exchange contributes a single power of the Coulomb's constant, $k_e = 1/(4\pi\epsilon_0)$, together with a distance dependence, R^{-3} , *i.e.* $(k_e R^{-3})^m$. Explicitly, conventional Raman scattering has zero exchanges and thus $m=0$; couplings (i) to (iv) engage a single virtual photon, $m=1$; (v) to (viii) engage two, $m=2$. The ensuing products in equation (1) can thus have inverse power distance dependences running up to R^{-12} .

III. MOLECULAR VIBRATIONS AND TENSOR STRUCTURES

In general, to discern the selection rules engaged by any specific molecular response tensor, the symmetries in the radiation modes must be identified. Most notable are the cases where two photon interactions are treated through identical radiation operators, and each of the cases introduced above may indeed have index symmetry resulting from such symmetry. Approximate index symmetries can also be seen in the case of two photons engaged in the Raman creation and annihilation events, analogous to the Placzek treatment for single-center scattering distant from resonance:²⁰ essentially, the assumption rests on the very different typical magnitudes of the electronic and vibrational transition energies.

Our interest lies in the vibrational transition from an initial state ψ_0 to a final state ψ_α occurring at molecule A, denoted by an " $\alpha 0$ " superscript on the respective molecular response tensor. The complete Born-Oppenheimer development for a rank 2 tensor can be found in the preceding paper (Subsection II C);⁵ here we extract the salient result. The molecular response tensors of each rank are developed in the same way using the Placzek treatment, in which the symmetry properties and selection rules are determined by the derivatives of the tensor, with respect to each vibrational coordinate Q , about the equilibrium position Q_0 . In the instance of the familiar vibrational transition polarizability tensor, where there is no overall change in electronic state, the leading non-zero term that accommodates a vibrational transition is the second in the Taylor series expansion;

$$\alpha_{ij}^{\alpha 0} \approx \langle \psi_\alpha | (Q - Q_0) | \psi_0 \rangle \left. \frac{\partial \alpha_{ij}^{00}}{\partial Q} \right|_{Q_0} + \dots \quad (2)$$

A non-zero Dirac bracket ensures that the dominant transitions are those that involve one quantum of vibrational energy.

In general terms, for the theory to be equally applicable under near-resonance conditions, the Raman polarizability would acquire a damping term in its energy denominators and the tensor would as a result lack any index symmetry. However, given the more common off-resonance conditions, it is well known that the antisymmetric part of the tensor essentially vanishes (a more detailed discussion of how this works is given in ref. ²¹).

From here onwards, all such index symmetries will be represented by sets of parentheses collecting the appropriate Cartesian indices, resulting in a Raman tensor represented as $\alpha_{(ij)}^{\alpha 0}$. Similar methods can be applied to all eight forms of coupling and the resultant response tensors and key characteristics will now be summarized. All of those that engage the same number of photon interactions will elicit a response designated by the same Greek character; for example two-photon processes are all characterized by an α .

The specific form of each tensor involved in the various forms of coupling can be retrieved from our previous study.⁵ They are long and complicated expressions, whose detail would be required in any calculations to quantify their relative contributions for particular molecules. As we shall see, it suffices here to summarize their form of participation. If we focus on the molecule of spectroscopic interest, molecule A where vibrational transitions occur, we can recognize that the couplings (i), (ii) and (viii) engage response tensors of these forms: $\alpha'_{(jk)}{}^{\alpha 0 A}$, $\alpha''_{(it)}{}^{\alpha 0 A}$ and $\chi''_{(ij)(km);(ln)}{}^{\alpha 0 A}$, respectively. The three forms of coupling (iii), (v) and (vi) that conform to three-photon selection rules generate $\beta''_{(ij)k}{}^{00 A}$, $\chi'_{jkm;iln}{}^{\alpha 0 A;00 B'}$ and $\chi''_{jkm;iln}{}^{\alpha 0 A}$, respectively. There is only one instance, (vii), where four-photon selection rules are engaged; $\chi_{(ij)(km);(ln)}{}^{\alpha 0 A;00 B}$. The one other possibility is the coupling case (iv), in which the molecule undergoes a single-photon process and therefore engages a vibrational transition moment $\mu_i^{\alpha 0 A}$.

IV. SYMMETRY ANALYSIS

Next, it is necessary to generalize the procedure required to identify the selection rules for molecular transitions, based on the terms listed in character tables,²² to enable identification of the vibrational symmetries that each tensor form allows. The origin of these rules lies in mapping the basis representations for a sphere on to point groups of lower symmetry, as determined by molecular structure. The most transparent and effective means of the appropriate eliciting selection rules is thus to resolve the associated molecular response functions into irreducible Cartesian tensors, each of which has a readily resolved symmetry behavior.

By way of simple illustration, we first review the analysis for $\alpha_{(\lambda\mu)}^{\alpha 0}$, where the subscript indices are now represented by Greek characters to denote Cartesian components referred to an axial framework for the molecule. Any such even-parity and index-symmetric second rank tensor is expressible as a sum of two irreducible parts, these transforming as a *scalar* (designated *weight* 0) and a symmetric traceless second rank tensor (*weight* 2). The decomposition can be written explicitly as follows;

$$\alpha_{(\lambda\mu)}^{\alpha 0} \equiv \alpha_{(\lambda\mu)}^{(0)} + \alpha_{(\lambda\mu)}^{(2)} \quad (3)$$

where the weights are indicated by the superscript numerals. An additional weight 1 term arises only when the input optical frequency approaches resonance. In all other cases the leading term from Equation (2) entails the following derivatives with weights $j = 0, 2$;

$$\left. \frac{\partial \alpha_{\lambda\mu}^{(j)}}{\partial Q} \right|_{Q_0}, \quad (4)$$

for clarity dropping essentially redundant state characters from the superscript. Each of the tensors that arise in the present analysis of coupling effects is developed to identify its dependence on vibrational transition in the same way as the transition polarizability is established for conventional Raman scattering.

In general a response tensor of rank n is deconstructed into a sum of irreducible tensors, each of rank n but distinguished by individual weights in the interval, $0 \leq j \leq n$. According to the specific details of the case in view, the individual terms may sometimes be null for certain values of j , whilst for other j values more than one irreducible tensor may feature in the sum. Generally, we can write;²³⁻³⁵

$$T_{i_1 \dots i_n} = \sum_{j=0}^n T_{i_1 \dots i_n}^{(j)} = \sum_{j=0}^n \sum_{p=1}^{N_n^{(j)}} T_{i_1 \dots i_n}^{(j;p)}, \quad (5)$$

where p is a seniority index, which is the number of occurrences, $N_n^{(j)}$ with which a given weight occurs. The highest weight n term, which only ever features once in the sum, has the transformation properties of a tensor of rank n that is symmetric and traceless with respect to every pair of indices, and is known as a *natural tensor*. It has $(2j + 1)$ independent components. In general, a weight p contribution can be considered a natural tensor of rank p embedded in rank n Cartesian space. The weight zero term or terms, if present, have the transformation properties of a scalar, and therefore always transforms under the totally symmetric representation of the molecular point group.

When index symmetry is introduced it reduces the number of linearly independent irreducible constituents; this accords with the fact that, for a Cartesian tensor of rank n , the number of linearly independent tensor components becomes less than 3^n . Indeed we have already seen how $j = 1$ term generally vanishes from the polarizability, consistent with a reduction from nine to six independent tensor components. In general if P denotes the number of independent components then it follows that we have;³⁶

$$P = \sum_{j=0}^n N_n^{(j)} (2j + 1). \quad (6)$$

Table I provides the details required for all the tensor forms that arise in the present analysis.


TABLE I. The complete set of irreducible weights $0 \leq j \leq 4$ for an arbitrary three-dimensional Cartesian tensor \mathbf{T} , of rank denoted by the number of subscript indices $1 \leq n \leq 4$. The presence of parentheses indicates symmetry in the relevant Cartesian indices. The second column gives total number of independent components, P .

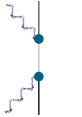
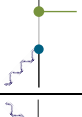

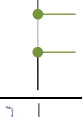

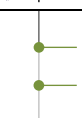
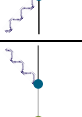
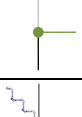
	P	$N_n^{(0)}$	$N_n^{(1)}$	$N_n^{(2)}$	$N_n^{(3)}$	$N_n^{(4)}$
T_λ	3	0	1			
$T_{\lambda\mu}$	9	1	1	1		
$T_{(\lambda\mu)}$	6	1	0	1		
$T_{\lambda\mu\nu}$	27	1	3	2	1	
$T_{(\lambda\mu)\nu}$	18	0	2	1	1	
$T_{(\lambda\mu)(\nu\sigma)}$	36	2	1	3	1	1

In Table I the number of subscripts corresponds to the rank of the process. As such, a rank 1 tensor (a vector) of the form T_λ , is expressed in one-photon processes at molecule A, as in the coupling case (iv). The entries for $T_{(\lambda\mu)}$ account for the symmetry of all rank 2 cases away from resonance, whilst for comparison $T_{\lambda\mu}$ is the symmetry of the tensors such as the transition polarizabilities (α) near resonance. The cases $T_{\lambda\mu\nu}$ and $T_{(\lambda\mu)\nu}$ are both symmetries seen in three-interaction processes; tensors of the form $T_{(\lambda\mu)(\nu\sigma)}$ arise from four interactions.

For the symmetry analysis that is to be our focus, a substantial simplification can now be effected. Although the full rate equations entail the detailed form of each of the molecular response tensors introduced in our previous paper,⁵ all of the symmetry information necessary to determine the modified Raman selection rules can be captured in simple icons as displayed in Table II – essentially the ‘left-hand sides’ of the Feynman diagrams in Fig. 1. The Table accounts for all the forms of coupling that arise, sorted by the number of interactions with molecule A. In each case the associated coupling tensor accommodates all of the weights that are displayed in the final column (as determined by Table I). The superscript on the rank denotes the parity of the interactions; for this work, each interaction is assumed to engage an electric dipole transition, and thus each additional interaction introduces a change in parity.

TABLE II. List of molecular response tensors with their corresponding forms of coupling, designated ‘case’, and the world-line for molecule A, sorted by rank, representing the number of interactions and noting the parity. Each of the permissible weights, ($0 \leq j \leq 4$) are displayed for the respective response tensors.

Rank	Case	Diagram	Tensor	Weights
1 ⁻	(iv)		$\mu_i^{\alpha 0A}$	(1)

2^+			$\alpha_{(ij)}^{\alpha 0}$	$(02)^a$
(i)		$\alpha'_{(jk)}{}^{\alpha 0,A}$	$(02)^a$	
(ii)		$\alpha^m_{(il)}{}^{\alpha 0,A}$	$(02)^a$	
(viii)		$\chi_{(ij)(km);(ln)}^{\alpha 0,B';\alpha 0,A}$	(02)	
3^-			$\beta_{(ij)k}^{00,A}$	(123)
(v)		$\chi'_{jkm;iln}{}^{\alpha 0,A;00,B'}$	(0123)	
(vi)		$\chi^m_{jkm;iln}{}^{\alpha 0,B;00,A'}$	(0123)	
4^+			$\chi_{(ij)(km);(ln)}^{\alpha 0,A';00,B}$	(01234)

^aNear resonance, these instances will include weight 1 components.

The addition of weight 1 for the transition polarizabilities, α , arises from the aforementioned reduction in symmetry under near-resonance, and is included only to allow for any additional vibrational lines that arise in the Raman spectrum under such conditions. Focusing on off-resonance effects, all cases with a two-photon process involving weight 0 or 2 in a tensor of rank and parity 2^+ will only arise under the same conditions in which conventional Raman scattering occurs; couplings of the form (i), (ii) and (viii) follow such a scenario and, as a result, are not the main interest of this work (since in these cases, no additional vibrational features will appear on the ensuing Raman spectra). To classify the other cases of specific interest the following table introduces a category system, referred to as ‘type’ in Table III, into which each and every *irrep* (irreducible representation) will fall: see Table IV of the Appendix.

TABLE III. Categorizes the *irreps* for all novel (neighbor-induced) Raman transitions according to the irreducible weights engaged.

Type	Rank 1 ⁻	Rank 3 ⁻		Rank 4 ⁺
	(1) ^a	(0123) ^b	(123) ^c	(01234) ^d
I	✓	✓	✓	✓
II	✓	✓	✓	
III	✓			✓
IV		✓	✓	✓
V		✓	✓	
VI			✓	✓
VII			✓	
VIII				✓

Engaged by corresponding forms of coupling: ^a (iv); ^b (iii); ^c (v) and (vi); ^d (vii).

V. ILLUSTRATIVE SPECTRAL MODES

In this section we offer an example of how the primary results, tabulated in the Appendix, can be deployed when interrogating the Raman spectra with neighbor-modified features. The case of benzene, briefly introduced in Subsection II G. of the previous paper,⁵ draws out many of the most salient properties and is further developed here. By inspecting the results for the symmetry group of benzene, D_{6h} , it is clear that there are 9 (out of 12) *irreps* that are conventionally disallowed in Raman scattering. By virtue of neighbor interaction, vibrational modes belonging to any of these *irreps* should evidently become observable in the Raman spectrum. One can envisage a mixture of benzene with low concentrations of an inert molecule, naphthalene for example, and the interactions between the pair should allow for the aforementioned additional interactions to be elicited. The three *gerade irreps* listed (A_{2g} , B_{1g} and B_{2g}) would all become allowed by the pathway of case (vii). A_{1u} , B_{1u} and E_{2u} all become allowed by virtue of cases (iii), (v) and (vi): the complete set of three photon interactions on molecule A. Moreover, A_{2u} and E_{1u} both engage all of cases (iii) through (vi), which are all of the odd ranked processes considered. It is noteworthy that naphthalene mixed with low concentrations of benzene should also exhibit additional Raman active lines. Naphthalene, of D_{2h} symmetry, should then display four additional classes of lines in its Raman vibrational spectra. This example is, of course, given only to exemplify the mechanisms at work and their potential consequences. Real systems, subjected to this kind of analysis, will need to take account of relative concentrations and avoid any possibility of weak association forces.

VI. CONCLUSION

In the work described above we have further developed our comprehensive research on various means by which neighbor-induced electronic interactions, between molecules in the condensed phase mixtures, can result in a modification of Raman spectra – even in systems without any significant chemical association between the components. The most interesting aspect is undoubtedly the possibility of generating new spectral lines,

corresponding to the engagement of normally forbidden molecular vibrations in Stokes transitions. Our previous work has shown that the relative strength of such lines, compared to normal lines in the Raman spectrum, can be estimated by the comparative magnitudes of the polarizability volume relative to the cube of the typical intermolecular separation between neighbors.

By focusing on the structural form of the various response tensors that feature in the previously derived results, and subjecting them to a scheme for irreducible tensor reduction, the present study has elicited a raft of new selection rules, directly reflecting the nature of the underlying mechanisms. The appearance of new lines in the Raman spectrum, as a result of neighbor interactions, is anticipated to be most evident in molecules of relatively high symmetry. It has been shown how to identify the possible symmetry types for molecular vibrations, conventionally forbidden by Raman selection rules, which may be responsible for such new lines. Care has been taken to distinguish between near-resonance and off-resonance forms of scattering. It is hoped that this research, along with our previous mechanistic analysis, will assist in the interpretation of weak spectral features in the Raman spectra of mixtures.

ACKNOWLEDGEMENTS

The authors thank the University of East Anglia (UEA) for funding this research.

APPENDIX: COMPLETE SET OF ADDITIONAL RAMAN ACTIVE IRREDUCIBLE REPRESENTATIONS

TABLE IV. Listing of *irreps* (for each point group) that relate to the spectral lines that may feature on a Raman spectrum with neighbor-modified features.

Point group	<i>Irrep</i>	Rank 1 ⁻	Rank 3 ⁻	Rank 4 ⁺	Type
C_i	A_u	1	0123		II
C_6	B		3	34	IV
S_6	A_u	1	0123		II
	E_u	1	123		II
S_8	B	1	0123	4	I
	E_1	1	123	34	I
S_{10}	A_u	1	0123		III
	E_{1u}	1	123		II
	E_{2u}		23		V
C_{2h}	A_u	1	0123		II
	B_u	1	123		II
C_{3h}	A''	1	0123	34	I
C_{4h}	A_u	1	0123		II
	B_u		23		V

	E_u	1	123		II
C_{5h}	E'_1	1	123	4	I
	A''	1	0123		II
	E''_2		23	34	IV
C_{6h}	B_g			34	VIII
	A_u	1	0123		II
	B_u		3		V
	E_{1u}	1	123		II
	E_{2u}		23		V
C_{3v}	A_2		023	134	IV
C_{4v}	A_2		02	134	IV
C_{5v}	A_2		02	13	IV
C_{6v}	A_2		02	13	IV
	B_1		3	34	IV
	B_2		3	34	IV
D_3	A_2	1	13	134	I
D_4	A_2	1	13	134	I
D_5	A_2	1	13	13	I
D_6	A_2	1	13	13	I
	B_1		3	34	IV
	B_2		3	34	IV
D_{2h}	A_u		023		V
	B_{1u}	1	123		II
	B_{2u}	1	123		II
	B_{3u}	1	123		II
D_{3h}	A'_2		3	13	IV
	A''_1		02	34	VIII
	A''_2	1	13	34	I
D_{4h}	A_{2g}			134	VIII
	A_{1u}		02		V
	A_{2u}	1	13		II
	B_{1u}		23		V
	B_{2u}		23		V
	E_u	1	123		II
D_{5h}	A'_2			13	VIII
	E'_1	1	123	4	I
	A''_1		02		V
	A''_2	1	13		II
	E''_2		23	34	IV
	A_{2g}			13	VIII

D_{6h}	B_{1g}		34	VIII	T_h	E_u		2	V		
	B_{2g}		34	VIII		T_u	1	123	II		
	A_{1u}	02		V	T_d	A_2		0	3	VI	
	A_{2u}	1	13			T_1		23	134	IV	
	B_{1u}		3		O	A_2		3	3	IV	
	B_{2u}		3			T_1	1	13	134	I	
	E_{1u}	1	123			O_h	A_{2g}		3	VIII	
	E_{2u}		23		V		T_{1g}		134	VIII	
D_{2d}	A_2		23	134	IV	A_{1u}		0	VII		
D_{3d}	A_{2g}		13	134	IV	A_{2u}		3	V		
	A_{1u}		023		V	E_u		2	V		
	A_{2u}	1	13		II	T_{1u}	1	13	II		
	E_u	1	123		II	T_{2u}		23	V		
D_{4d}	A_2	1		13	III	I	T_1	1	1	1	I
	B_1		02	4	IV		T_2		3	3	IV
	B_2	1	13	4	I		G		3	34	IV
	E_1	1	123	34	I	I_h	T_{1g}		1	VIII	
D_{5d}	A_{2g}			13	VIII		T_{2g}		3	VIII	
	A_{1u}		02		V		G_g		34	VIII	
	A_{2u}	1	13		II		A_u		0	VII	
	E_{1u}	1	123		II		T_{1u}	1	1	II	
	E_{2u}		23		V		T_{2u}		3	V	
D_{6d}	A_2			13	VIII		G_u		3	V	
	B_1		02		V		H_u		2	V	
	B_2	1	13		II						
	E_1	1	123		II						
	E_3		3	34	IV						
	E_4		23	4	IV						
	$C_{\infty v}$	Σ^-		02	13	IV					
Φ			3	34	IV						
Γ				4	VIII						
$D_{\infty h}$	Σ_g^-			13	VIII						
	Φ_g			34	VIII						
	Γ_g			4	VIII						
	Σ_u^+	1	13		II						
	Σ_u^-		02		V						
	Π_u	1	123		II						
	Δ_u		23		V						
	Φ_u		3		V						
	A_u		03		V						

REFERENCES

- S. Marqués-González, R. Matsushita, and M. Kiguchi, *J. Opt.* **17**, 114001 (2015).
- C. H. Camp Jr and M. T. Cicerone, *Nat. Photonics* **9**, 295 (2015).
- F. Zapata, M. López-López, and C. García-Ruiz, *Appl. Spectrosc. Rev.* **51**, 227 (2016).
- C. Krafft, I. W. Schie, T. Meyer, M. Schmitt, and J. Popp, *Chem. Soc. Rev.* **45**, 1819 (2016).
- M. D. Williams, D. S. Bradshaw, and D. L. Andrews, *J. Chem. Phys.* **144**, 174304 (2016).
- D. P. Craig and T. Thirunamachandran, *Molecular Quantum Electrodynamics* (Academic Press, London, 1984).
- A. Salam, *Molecular Quantum Electrodynamics: Long-Range Intermolecular Interactions* (Wiley, Hoboken, NJ, 2010).
- A. Salam, *J. Chem. Phys.* **122**, 044112 (2005).
- A. Salam, *J. Chem. Phys.* **124**, 014302 (2006).
- A. Salam, *J. Chem. Phys.* **136**, 014509 (2012).
- J. E. Frost and G. A. Jones, *New J. Phys.* **16**, 113067 (2014).
- P. W. Milonni and S. M. H. Rafsanjani, *Phys. Rev. A* **92**, 062711 (2015).
- X. Liu and J. Qiu, *Chem. Soc. Rev.* **44**, 8714 (2015).

- ¹⁴ D. Weeraddana, M. Premaratne, and D. L. Andrews, *Phys. Rev. B* **92**, 035128 (2015).
- ¹⁵ M. D. LaCount, D. Weingarten, N. Hu, S. E. Shaheen, J. van de Lagemaat, G. Rumbles, D. M. Walba, and M. T. Lusk, *J. Phys. Chem. A* **119**, 4009 (2015).
- ¹⁶ M. D. LaCount and M. T. Lusk, *Phys. Rev. A* **93**, 063811 (2016).
- ¹⁷ D. L. Andrews and D. S. Bradshaw, *Ann. Phys. (Berlin)* **526**, 173 (2014).
- ¹⁸ N. J. Dawson, B. R. Anderson, J. L. Schei, and M. G. Kuzyk, *Phys. Rev. A* **84**, 043407 (2011).
- ¹⁹ G. E. Stedman, *Diagram Techniques in Group Theory* (Cambridge University Press, Cambridge, UK, 1990).
- ²⁰ G. Placzek, *Handbuch der Radiologie* (Akademische Verlag, Leipzig, Germany, 1934), Vol. 6, part 2.
- ²¹ D. L. Andrews and J. S. Ford, *J. Chem. Phys.* **139**, 014107 (2013).
- ²² J. A. Salthouse and M. J. Ware, *Point Group Character Tables and Related Data* (Cambridge University Press, London, 1972).
- ²³ J. A. R. Coope, R. F. Snider, and F. R. McCourt, *J. Chem. Phys.* **43**, 2269 (1965).
- ²⁴ J. A. R. Coope and R. F. Snider, *J. Math. Phys.* **11**, 1003 (1970).
- ²⁵ J. Jerphagnon and S. K. Kurtz, *J. Appl. Phys.* **41**, 1667 (1970).
- ²⁶ H. Jeffreys, *Math. Proc. Camb. Phil. Soc.* **73**, 173 (1973).
- ²⁷ R. A. Harris, W. M. McClain, and C. F. Sloane, *Mol. Phys.* **28**, 381 (1974).
- ²⁸ A. J. Stone, *Mol. Phys.* **29**, 1461 (1975).
- ²⁹ J. Jerphagnon and D. S. Chemla, *J. Chem. Phys.* **65**, 1522 (1976).
- ³⁰ J. Jerphagnon, D. Chemla, and R. Bonneville, *Adv. Phys.* **27**, 609 (1978).
- ³¹ D. S. Chemla and R. Bonneville, *J. Chem. Phys.* **68**, 2214 (1978).
- ³² D. L. Andrews and W. A. Ghoul, *Phys. Rev. A* **25**, 2647 (1982).
- ³³ D. L. Andrews and N. P. Blake, *J. Phys. A: Math. Gen.* **22**, 49 (1989).
- ³⁴ J. Zyss, *J. Chem. Phys.* **98**, 6583 (1993).
- ³⁵ S. R. Mane, *Nucl. Instr. Meth. Phys. Res. A* **813**, 62 (2016).
- ³⁶ D. L. Andrews, *Spectrochim. Acta, Part A* **46**, 871 (1990).